Mechatronics 57 (2019) 140–149

Contents lists available at ScienceDirect

Mechatronics

journal homepage: www.elsevier.com/locate/mechatronics

A study on actuator delay compensation using predictive control technique with experimental verification☆

Asal Nahidi[a,*], Amir Khajepour[a], Alireza Kasaeizadeh[b], Shih-Ken Chen[b], Bakhtiar Litkouhi[b]

[a] Department of Mechanical and Mechatronics Engineering, University of Waterloo, Waterloo, ON N2L 3G1, Canada
[b] General Motors LLC. Warren, MI 48090, USA

ARTICLE INFO

Keywords:
Model predictive control
Actuator dynamic delay
Differential braking
Real-time implementation
Low computational complexity
Simulation and experimental verifications

ABSTRACT

In this paper, a model predictive control (MPC) method for actuator delay compensation in vehicle stability control is presented. At each sampling time, an MPC controller computes required torque adjustments in order to follow desired vehicle dynamics on slippery road condition. Actuator delay in a control loop can diminish controller effectiveness to a great extent and may even engender instability in a critical driving situation. Two control structures with different computational complexities are presented. In the first approach, the MPC problem is formulated such that actuator dynamics is considered in prediction model. Whereas, the second approach investigates actuator lag impact on control action allocation (distribution) through a transfer matrix. In contrast to common delay handling approaches, the proposed method is simply real-time implementable and does not necessitate an intricate design procedure. The complication of model predictive controller remains intact, since online computation load is not substantially altered. Discussions are presented on computational burden and performance of two control schemes using computer-aided simulations in MATLAB/CarSim environment as well as experiments. A rear-wheel-drive sport utility vehicle equipped with differential braking is utilized for numerical simulations and experimentations. According to the simulation results, success of the proposed method in tackling actuator delay in vehicle stabilization is inquired. Experimental tests also demonstrate competency of the proposed technique. Although this technique is applied to a vehicle stability control with a particular actuator, it is not limited to a certain set of problems and can be employed for a broad variety of actuators or more generally, model predictive control problems with actuator identifiable time delays.

1. Introduction

Recent developments in vehicle stability control depicts an ever-increasing trend in assisting traffic incidents reduction. A key reason to incident occurrence is complicated nonlinear vehicle response in critical driving situations such as high speeds and low traction roads. In these situations, a driver may not be successful in controlling the vehicle at stability margin based on her/his everyday driving experience. For safety enhancement, researchers devoted a serious effort to design Advanced Vehicle Safety Controllers (AVSC) to contribute in challenging driving scenarios. Anti-lock Braking System (ABS), Traction Control System (TCS), and Electronic Stability Control (ESC) have been emerged to facilitate directional stability and better vehicle handling performance [1]. Many market vehicles nowadays have different safety features that interpret signals from various sensors and calculate required control adjustments. A considerable improvement has been achieved in stability control technologies hitherto; nevertheless, supplementary investigation is still required to an ultimate goal of no accident due to human error [2,3]. Among all forms of optimal control algorithms, model predictive control (MPC) has received a lot of attention in latest decades. The outstanding specification of MPC technique is that it allows explicit constraint treatment in controller design [4]. In this control algorithm, a mathematical description (model) of a system is employed to predict its dynamic behavior over a finite horizon of time [5]. Then, a set of control actions are computed through solving an optimization problem to consider the impacts of adjustments on system behavior in control period. The MPC prediction model plays a significant role in closed loop performance of the controller. The prediction model should be sufficiently precise to capture the most significant dynamics of a system, and concurrently simple enough for real-time implementation [6]. Linear prediction models are less costly in application; however, nonlinear models provide a more accurate anticipation in a wider vehicle operation scope [7,8]. As global dynamics of a system can be described better with a nonlinear model, some research works were conducted to

☆ This paper was recommended for publication by Associate Editor Prof. Junmin Wang.

* Corresponding author.
E-mail address: sanahidi@uwaterloo.ca (A. Nahidi).

https://doi.org/10.1016/j.mechatronics.2018.11.007
Received 29 January 2018; Received in revised form 8 September 2018; Accepted 18 November 2018

investigate nonlinear MPC. For instance, Falcone et al. proposed a model predictive control structure for path following of autonomous vehicles [9]. Two controllers are designed to fulfill obstacle avoidance objective based on a linear bicycle and nonlinear full vehicle models. The proposed controllers are compared in terms of performance and computational burden. It was illustrated that real-time implementation of the controller with linear model is feasible; whereas fair simulation assessments showed that the MPC optimization process with a full nonlinear model is very time-consuming and not applicable in real-time. Borrelli et al. investigated a nonlinear MPC control approach for autonomous vehicle stabilization through active steering constrained to actuator limitations [10]. This study was a part of ongoing internal Ford research activities where nonlinear MPC was first offered in [11], and it was then continued to be investigated for more specific purposes. These purposes can be summarized as increasing the stability region of the controlled system in comparison with linear controllers, examining computational burden of a nonlinear controller, and generating a baseline controller to compare its performance with sub-optimal controllers. Additionally, a minimum number of preview steps is presented for an acceptable performance at a certain speed. The proposed controller was tested using simulations only, where results depicted complex steering maneuvers such as double lane change could be controlled on snow-covered road with initial speed of 17 m/s. Although nonlinear MPC is superior in accuracy, feasibility of real-time implementation is the most decisive aspect in engineering practice. Thus, several studies have been conducted based on successive linearization of a nonlinear model to avoid dealing with nonlinear constrained optimization. Linearized MPC provides a sub-optimal feedback policy without requiring a costly computational resource. Canale et al. reduced the computational complexities of a nonlinear MPC with an efficient approximation method based on a set membership technique [4]. The performance of the controller was tested with software-in-the-loop simulations and was compared to a more accurate nonlinear model. The reported controller performance was satisfactory in comparison with the accurate nonlinear model; however, it is more advantageous over the nonlinear one due to its real-time implementation practicability. They also investigated the stability and constraint satisfaction of the proposed controller in control demanding conditions. The stability analysis demonstrated that the controller is able to handle a system with constraints and model uncertainties in a systematic way. Bemporad and Rocchi applied a hierarchical linear time-varying MPC approach on unmanned aerial vehicles and considered constraints such as motor thrust, vehicle angle and position, and collision avoidance in optimization [12]. This approach utilizes a simplified dynamic model of a stable vehicle as well as a novel convex approximation of achievable states. Simulation results illustrated a satisfactory level of performance in comparison with more complicated hybrid prediction models with a minor performance sacrifice and less computational complexity. Some similar research works are presented in [13] and [14].

All controllers with any control technique are susceptible to performance deterioration in case of delay existence in the control cycle. The origin of the delay can be from numerous sources such as control action computation, sensory communication, measurement, or actuation system. In model predictive control approach, more computation entails a significant processing time and results in a larger accumulated delay in the control cycle. Cortes et al. proposed a model predictive current control with delay compensation of a three-phase power inverter [15]. The delay is compensated using a simple solution that reflects the calculation time and estimates current in the next sampling time. Computer simulation and experimental results were presented to show the usefulness of the delay compensation approach. According to the experimental results, the number of current ripples are decreased noticeably. Su et al. studied elimination of potential computational process delay in a robust MPC controller [16]. As robustness requires a fast sampling rate setting to respond to uncertainties, a dual time-scale control structure is introduced for computational delay mitigation. In this control structure, first, a pre-compensator unit works with a high sampling frequency to overcome uncertainties, while the MPC unit employs a lower sampling rate in control action calculation. Stability and feasibility analyses were presented for the proposed scheme. The control approach is validated using simulations. Liu et al. presented an MPC controller for obstacle avoidance in unmanned ground vehicles with significant dynamics [17]. In this study, sensor data attainment, communication, and processing delays as well as computation, control action transmission or actuator delays are lumped into sensing and control delays, respectively. The sensing delay is introduced as LIDAR data utilized at the current time and measured in T_{ds} seconds ago, whereas the control delay means that the command will not be applied to the system until T_{dc} seconds later. The constraints for obstacle avoidance were reformulated by analyzing sensing delay. The control delays were taken into account with a time shift in prediction model. Simulation outcomes indicated a satisfactory performance with proposed controller at different sensing and control delays and vehicle speeds.

The main contributions of this paper are presenting a predictive technique to tackle actuator delays in model predictive control framework. As the command and delivered control actions may be different at each sampling time due to actuator dynamics, this model proposes a remedy to remove the effect of such a delay in the closed loop performance. The most advantageous features of the proposed method is generality of the actuator delay handling approach and no significant change in computational complexity. The prediction model only encompasses vehicle dynamics model and actuator model is considered in the distribution level through a transfer matrix that is estimated at each sampling time. The result is a real-time implementable model predictive control scheme that foresees the vehicle body and actuator dynamics evolution in a certain prediction horizon to calculate a precise control action with delay compensation algorithm. The capability of the proposed technique is verified through software simulations using CarSim and MATLAB. Furthermore, experimental results are presented with a GM Equinox to evaluate the performance of the suggested technique in real-time. This paper is organized as follows: Section 2 includes prediction model, cost function, and constraints of baseline and proposed model predictive controllers for vehicle stabilization. Additionally, the proposed delay handling technique is formulized and presented. Section 3 shows simulation results obtained using two controllers, and some experimental tests are illustrated in Section 4. The summary of the findings of this research are reported in Section 5.

2. Controller design

In this section, two model predictive controllers are designed and compared to each other. The main objective is enhancing vehicle handling (steerability) response and maintaining lateral stability despite of actuator dynamic delay in different driving scenarios. Both controllers receive feedback from the vehicle and determine the optimal torque adjustments δQ for desired yaw rate and lateral velocity tracking purposes. Then, the torque adjustments are added to the driver torque command, and applied to vehicle via a four-wheel-independent brake system. Note that generated torque by the actuator is a differential negative one at each corner. The actuator dynamic delay is mathematically modeled in prediction model of controller A, whereas in controller B, the effect of delay is considered on control adjustment distribution for less computational burden. The design approach details of each controller is presented in the rest of this section.

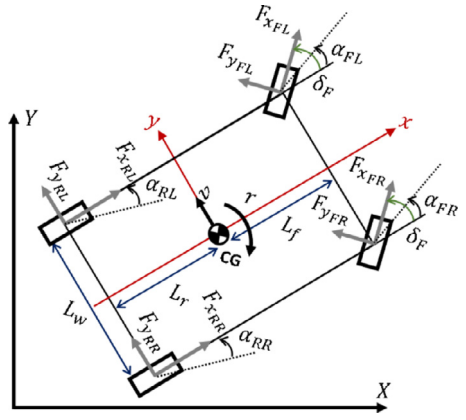

Fig. 1. Double-track vehicle model used as prediction model for controller A.

2.1. Desired yaw rate and sideslip responses

The desired yaw rate and lateral velocity responses of the vehicle is defined by [18]:

$$r^* = \delta_F u/\left(L + K_{us}u^2\right) \tag{1}$$

where δ_F is the front steering angle, u is the vehicle forward speed, L is the vehicle wheelbase, and K_{us} is understeer coefficient of the vehicle response. The achievable or feasible yaw rate has to be limited to the road condition. The maximum lateral acceleration can be utilized as a measure of road/tire grip coefficient. Thus, desired yaw rate on any road condition can be presented as:

$$r_{des} = \text{sign}(r^*) \times \min\left(|r^*|, \left|a_{y_{max}}/u\right|\right) \tag{2}$$

where $a_{y_{max}}$ is the achievable maximum lateral acceleration on a specific road surface. The desired lateral velocity can be defined based on the desired yaw rate as:

$$v_{des} = \tan\left(r_{des}\left(L_r - L_f m u^2\right)/\left(uL\left(C_{\alpha_f} + C_{\alpha_r}\right)\right)\right) \tag{3}$$

where L_f and L_r are distances of vehicle CG to front and rear axles, and C_{α_f} and C_{α_r} are cornering coefficients of front and rear tires. The calculated value for desired lateral velocity is usually very insignificant and mostly considered equal to zero.

2.2. Prediction model of controller A

A double-track vehicle model as shown in Fig. 1, is employed to forecast the vehicle lateral velocity and yaw rate responses as well as delivered torque adjustment over a prediction horizon. This model is competent enough to consider the effect of differential braking on state evolutions in future and captures the directional dynamics of the vehicle, notwithstanding it is real-time implementable. In addition to the vehicle model, a reasonably precise tire model is necessary to obtain an adequate accuracy of vehicle state prediction. In the MPC framework of controller A, the uncontrolled driver inputs such as brake/gas pedal positions and steering wheel angle are assumed to be unchanged during the course of prediction window. In this paper, the prediction model for controller A involves the following vehicle states:

$$X = \begin{bmatrix} v & r & \delta\bar{Q}_{FL} & \delta\bar{Q}_{FR} & \delta\bar{Q}_{RL} & \delta\bar{Q}_{RR} \end{bmatrix}^T \tag{4}$$

In this equation, v is the lateral velocity, r is the yaw rate, and $\delta\bar{Q}_{FL}$, $\delta\bar{Q}_{FR}$, $\delta\bar{Q}_{RL}$, and $\delta\bar{Q}_{RR}$ are front left, front right, rear left, and rear right delivered torque adjustment. In this study, it is assumed that an estimation module is available separately to the controller that provides estimated tire forces at each sampling time [19]. The cornering force variation is necessary to be considered for an accurate prediction of vehicle dynamic state evolutions within the prediction horizon. Using cornering coefficients, cornering tire forces can be written as:

$$F_{y_{ij}} = C_{\alpha_{ij}}\alpha_{ij} \quad i = F, R \text{ and } j = L, R \tag{5}$$

where $C_{\alpha_{ij}}$ is the cornering coefficient of the tire ij calculated by linearization of the tire model about the operating point, and α_{ij} is the slip angle of the tire ij. Traction tire forces can be approximated as $F_{x_{ij}} = Q_{ij}/R_{eff}$, where Q_{ij} is the total driver and controller torques applied on the wheel ij and R_{eff} is the effective wheel radius. The vehicle CG total cornering force F_Y and lateral velocity v can be expressed by a double-track model as:

$$F_Y = \sum_{i=F,R}\sum_{j=L,R}\left(F_{x_{ij}}\sin\delta_{ij} + F_{y_{ij}}\cos\delta_{ij}\right) \tag{6}$$

$$\dot{v} = F_Y/m - ur \tag{7}$$

The vehicle yaw moment G_Z and yaw rate r can also be imparted as:

$$\begin{aligned} G_Z = {} & L_f\sum_{i=F}\sum_{j=L,R}\left(F_{x_{ij}}\sin\delta_{ij} + F_{y_{ij}}\cos\delta_{ij}\right) \\ & -L_r\sum_{i=R}\sum_{j=L,R}\left(F_{x_{ij}}\sin\delta_{ij} + F_{y_{ij}}\cos\delta_{ij}\right) \\ & +L_w\sum_{i=F,R}\sum_{j=R}\left(F_{x_{ij}}\cos\delta_{ij} - F_{y_{ij}}\sin\delta_{ij}\right) \\ & -L_w\sum_{i=F,R}\sum_{j=L}\left(F_{x_{ij}}\cos\delta_{ij} - F_{y_{ij}}\sin\delta_{ij}\right) \end{aligned} \tag{8}$$

$$\dot{r} = G_Z/I_Z \tag{9}$$

In Eqs. (6)–(9) m is the total mass, I_Z is moment of inertia around normal axis, and L_w represents track width of the vehicle. The actuator dynamic delay is model through a first-order delay by considering the delivered torque adjustment $\delta\bar{Q}_{ij}$ as a state-variable in prediction model and the commanded torque adjustment δQ_{ij} as control input:

$$\delta\dot{\bar{Q}}_{ij} = T\left(\delta\bar{Q}_{ij} - \delta Q_{ij}\right) \qquad i = F, R \text{ and } j = L, R \tag{10}$$

where parameter T can be found as $T = 1/\tau$, and τ is the actuator time-constant. The input of the prediction model is the vector of braking torque adjustment to each wheel:

$$U = \begin{bmatrix} \delta Q_{FL} & \delta Q_{FR} & \delta Q_{RL} & \delta Q_{RR} \end{bmatrix}^T \tag{11}$$

The output of the controller A is the vehicle lateral velocity and yaw rate. At each sampling time Eqs. (6)–(10) are utilized to predict the output based on the current measurements/estimation. The model inputs were introduced in Eq. (10). Thus, a standard state-space representation can be illustrated as:

$$\begin{cases} \dot{X} = AX + BU \\ Y = CX \end{cases} \tag{12}$$

where A, B, and C are system, input, and output matrices, respectively. In order to design an MPC based controller, the aforementioned matrices should be descried. The state-space system in Eq. (12) can be discretized using Step Invariant approximation to handle possible matrix singularities [20]:

$$\tilde{A} = I + EAT_s \tag{13}$$

$$E = \sum_{n=0}^{\infty}\left(AT_s\right)^n/(n+1)! \tag{14}$$

$$\tilde{B} = EBT_s \tag{15}$$

$$\tilde{C} = C \tag{16}$$

where $\tilde{A}$, $\tilde{B}$, and $\tilde{C}$ are discretized system, input, and output matrices, respectively. Moreover, T_s is control loop sampling time and I is identity matrix of a proper size.

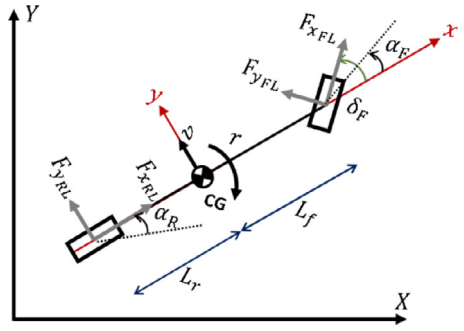

Fig. 2. Bicycle vehicle model used as prediction model for controller B.

2.3. Quadratic programming setup for controller A

The following performance index is considered for controller A to follow the desired lateral velocity and yaw rate:

$$J = \sum_{k=1}^{N} \left(\left\| Y_{des} - Y_k \right\|_Q^2 + \left\| +U_k \right\|_R^2 \right) \tag{17}$$

where N is the number of the prediction or control horizon. The first term in Eq. (17) is the lateral velocity and yaw rate tracking errors, and the second term minimizes control effort to achieve desired output values Y_{des}. Matrices Q and R are positive semi-definite and positive definite weight matrices of appropriate order, respectively. Two approaches can be employed to solve the problem described in Eq. (17); the first one is a recursive approach [21], and the second one is a batch approach that is used in this paper. According to batch approach, all the future steps of output $Y_{k+1}, Y_{k+2}, \ldots, Y_{k+N}$ are written based on the control input U and initial states Y_k . The intermediate states are eliminated due to successive substitution of previous states and control inputs up until initial states appear. Therefore, the performance index in Eq. (17) can be expressed as a quadratic function of $\bar{U} = [U_1 \quad U_2 \quad \ldots \quad U_k]^T$ vector of control interventions:

$$J = \bar{U}^T H \bar{U} + g\bar{U} + \text{const.} \tag{18}$$

where H is a symmetric positive definite matrix and is defined based on the weight matrix Q and R, as well as the prediction model. Furthermore, vector F is a function of initial state and the desired response. More details about these matrices can be found in [22].

2.4. Prediction model of controller B

The vehicle model used in controller B design is based on nonlinear bicycle model that describes the key components for vehicle handling control depicted in Fig. 2. This prediction model represents the lateral and yaw motion changes only, and a transfer matrix is used to fulfill actuator delay compensation. The transfer matrix mimics the time lag that should be taken into account in distribution regime. In general, the preferred model for controller B comprises less computational complexity for body dynamics prediction in comparison with controller A model. Similar to controller A, the driver commands such as brake/gas pedal positions and steering wheel angle are assumed to be constant for period of vehicle body dynamics forecast in MPC arrangement. In this paper, the following vehicle states are included in controller B prediction model:

$$X = \begin{bmatrix} v & r \end{bmatrix}^T \tag{19}$$

Similar to controller A, cornering forces can be calculated with a high precision at each sampling time using an estimation module and particular changes throughout the prediction horizon [23]. Eq. (5) is employed to obtain the tire cornering force variation. The vehicle CG total cornering force F_Y can be expressed by a bicycle model as:

$$F_Y = F_{y_R} + F_{y_F} \cos\delta_F + F_{x_F} \sin\delta_F \tag{20}$$

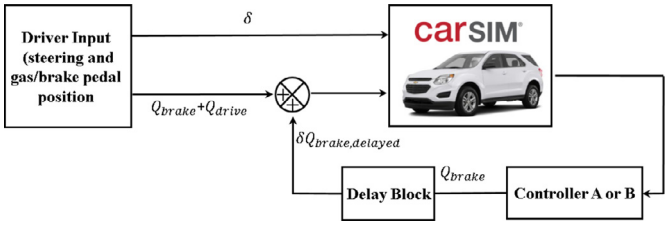

Fig. 3. Block diagram of the control structure in simulation.

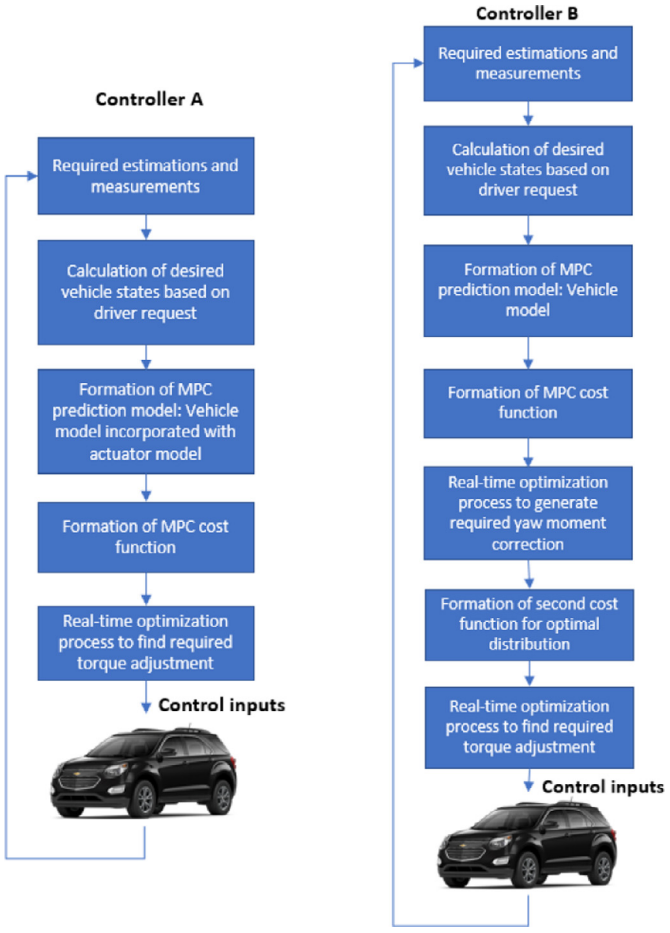

Fig. 4. Realtime control algorithm in controllers A and B.

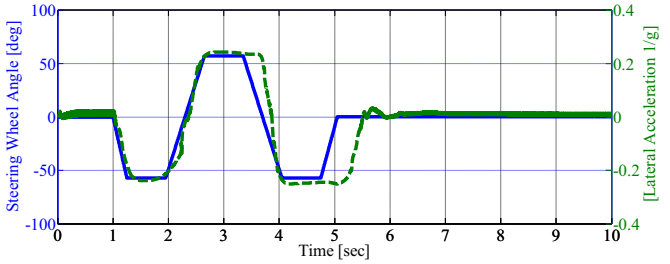

Fig. 5. Driver Steering command and lateral acceleration.

The lateral velocity v change can be assessed substituting Eq. (20) in Eq. (7). The vehicle yaw moment G_Z can also be declared as:

$$G_Z = L_f F_{y_F} \cos\delta_F - L_r F_{y_R} + L_f F_{x_F} \sin\delta_F \tag{21}$$

The yaw rate r change can be found by utilizing Eq. (21) in Eq. (9). The input of the prediction model is the vector of yaw moment adjust-

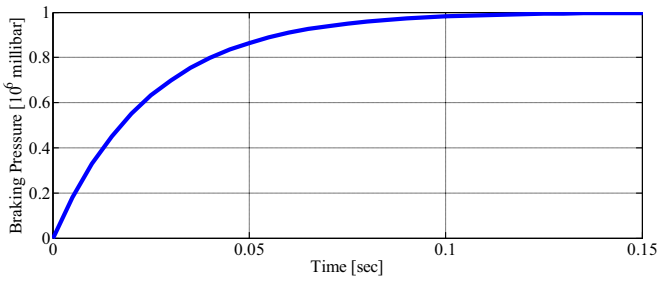

Fig. 6. Simulated brake system response to step input.

ment at vehicle center of gravity:

$$U = \left[\delta G_Z\right]^T \tag{22}$$

The output of the controller B is also the vehicle lateral velocity and yaw rate. Eqs. (19)–(22) are used to anticipate the output depending on the existing measurements/estimation. The model inputs were introduced in Eq. (22) resulting in a standard state-space form shown in Eq. (12). Resembling discretization method and sampling time are used to approximate matrices A, B, and C. The corresponding discretization equations are shown in Eqs. (13)–(16).

2.5. Quadratic programming setup for controller B

A reduced dimensional MPC is presented for controller B compared to controller A, where the control action is only yaw moment adjustment. In order to compensate the CG yaw moment error using differential braking torque, a distribution algorithm is required. In this paper, a multi-point holistic corner control approach is developed that allows investigating the impact of actuation system delay on the requested control action. Despite of original Holistic Corner Control (HCC) technique [24–26], the optimization process can be performed for multiple points belong to the control horizon. In the proposed technique, a transfer matrix as a compact description emulates actuator delay. A vector of required control actions for delay compensation are granted outcomes of optimization process. The CG yaw moment adjustment equals to discrepancies between desired (required) and actual (delivered) yaw moment, and can be written as:

$$\delta G_Z = G_{Z\,des} - G_Z\left(\mathcal{F} + \delta\mathcal{F}_1 + \delta\mathcal{F}_2 + \ldots + \delta\mathcal{F}_M\right) \tag{23}$$

where $G_{Z\,des}$ denotes CG desired yaw moment, $\mathcal{F} = [F_{x_{FL}} \quad F_{x_{FR}} \quad F_{x_{RL}} \quad F_{x_{RR}}]^T$ refers to corner longitudinal forces, and $\delta\mathcal{F}_k$ stands for corner longitudinal force adjustment vector at time i with control horizon of size M. Using Taylor series expansion and associated Jacobian matrix ∇G, right-hand side of Eq. (23) yields:

$$\nabla G = \partial G/\partial\mathcal{F} \quad k = 1,\ 2,\ \ldots,\ M \tag{24}$$

$$\begin{aligned} G_{Z\,des} - G_Z\left(\mathcal{F} + \delta\mathcal{F}_1 + \delta\mathcal{F}_2 + \cdots + \delta\mathcal{F}_M\right) &= G_{Z\,des} - G_Z(\mathcal{F}) - \nabla G\delta\mathcal{F}_1 \\ -\nabla G\delta\mathcal{F}_2 - \cdots - \nabla G\delta\mathcal{F}_M & \end{aligned} \tag{25}$$

To proceed distribution technique development, Eq. (25) can be rewritten as:

$$\begin{aligned} G_{Z\,des} - G_Z\left(\mathcal{F} + \delta\mathcal{F}_1 + \delta\mathcal{F}_2 + \cdots + \delta\mathcal{F}_M\right) &= \delta G_Z \\ -\nabla G \times \left(\delta\mathcal{F}_1 + \delta\mathcal{F}_2 + \cdots + \delta\mathcal{F}_M\right) & \end{aligned} \tag{26}$$

Dual optimization processes should be carried out at each sampling time to calculate essential control law. First, an MPC optimization with a similar performance index to the one shown in Eq. (17) should be performed, in which the output Y is identical for both controllers, but input U is yaw moment adjustment instead of braking torque adjustments in controller B. The result of MPC optimization problem next is exploited in the following performance index for corner optimal distribution:

$$P = \sum_{k=1}^{M}\left(\left\|\delta G_Z - \sum_{l=1}^{l=k}\nabla\mathcal{r}G_l\delta\mathcal{F}_l\right\|_S^2 + \left\|\delta\mathcal{F}_k\right\|_W^2\right) \tag{27}$$

where M is the number of the prediction or control horizons. In Eq. (27), $\mathcal{r}_l$ refers to time-domain response of actuator to unit-step matrix at time l, and can be calculated based on inverse Laplace Transform of calculated output based on the defined system transfer matrix and input. The first term in Eq. (27) minimizes CG yaw moment error, and the second component of the target function is to achieve the control goal with minimal control activity. Matrices S and W are positive semidefinite and positive definite weight matrices of appropriate order, respectively. Proper expansion of Eq. (27) results in a quadratic function of $\delta\bar{\mathcal{F}} = [\delta\mathcal{F}_1 \quad \delta\mathcal{F}_2 \quad \ldots \quad \delta\mathcal{F}_M]^T$ vector of control actions, as shown in Eq. (18). In this equation, Hessian matrix H can be obtained as:

$$H = \bar{H} + \bar{W} \tag{28}$$

in which

$$\bar{W} = \begin{bmatrix} W & 0 & 0 & \ldots & 0 \\ 0 & W & 0 & \ldots & 0 \\ 0 & 0 & W & \ldots & 0 \\ \vdots & \vdots & \vdots & \ddots & \vdots \\ 0 & 0 & 0 & \ldots & W \end{bmatrix} \text{ and}$$

$$\bar{H} = \begin{bmatrix} \bar{H}_{11} & \bar{H}_{12} & \bar{H}_{13} & \ldots & \bar{H}_{1M} \\ \bar{H}_{21} & \bar{H}_{22} & \bar{H}_{23} & \ldots & \bar{H}_{2M} \\ \bar{H}_{31} & \bar{H}_{32} & \bar{H}_{33} & \ldots & \bar{H}_{34} \\ \vdots & \vdots & \vdots & \ddots & \vdots \\ \bar{H}_{M1} & \bar{H}_{M2} & \bar{H}_{M3} & \ldots & \bar{H}_{MM} \end{bmatrix} \tag{29}$$

Elements of $\bar{H}$ can be found using definition of matrix $\mathcal{O}$ and $\in = |m - n|$ as follows:

$$\bar{H}_{mn} = \sum_{k=\mathcal{O}_{mn}}^{1}\left(\nabla G\mathcal{r}_k\right)S\left(\nabla G\mathcal{r}_{k+\in}\right)^T \tag{30}$$

$$\mathcal{O} = \begin{bmatrix} M & M-1 & M-2 & \ldots & 1 \\ M-1 & M-1 & M-2 & \ldots & 1 \\ M-2 & M-2 & M-2 & \ldots & 1 \\ \vdots & \vdots & \vdots & \ddots & \vdots \\ 1 & 1 & 1 & \ldots & 1 \end{bmatrix} \tag{31}$$

In addition to H, vector g can be presented as:

$$g = \begin{bmatrix} g_1 & g_2 & \cdots & g_M \end{bmatrix}^T \tag{32}$$

where the elements of F can be found as:

$$g_n = \sum_{k=M-n+1}^{1}\delta G_Z W\nabla G\,\mathcal{r}_k \tag{33}$$

2.6. Optimization constraints

In this paper, the auction system that is used for simulation and experimental validations is differential braking system that has a limitation on the amount of generatable negative torque on wheels. This limit is a mechanical characteristic of any brake system (i.e. electromagnetic, hydraulic, air, etc.) and typically varies with number of pads. The limits on the control actions due to this capacity can be expressed as:

$$lb = Q_{brake}^{max} \tag{34}$$

$$ub = 0 \tag{35}$$

$$LB = \begin{bmatrix} lb^T & lb^T & \cdots & lb^T \end{bmatrix}^T \tag{36}$$

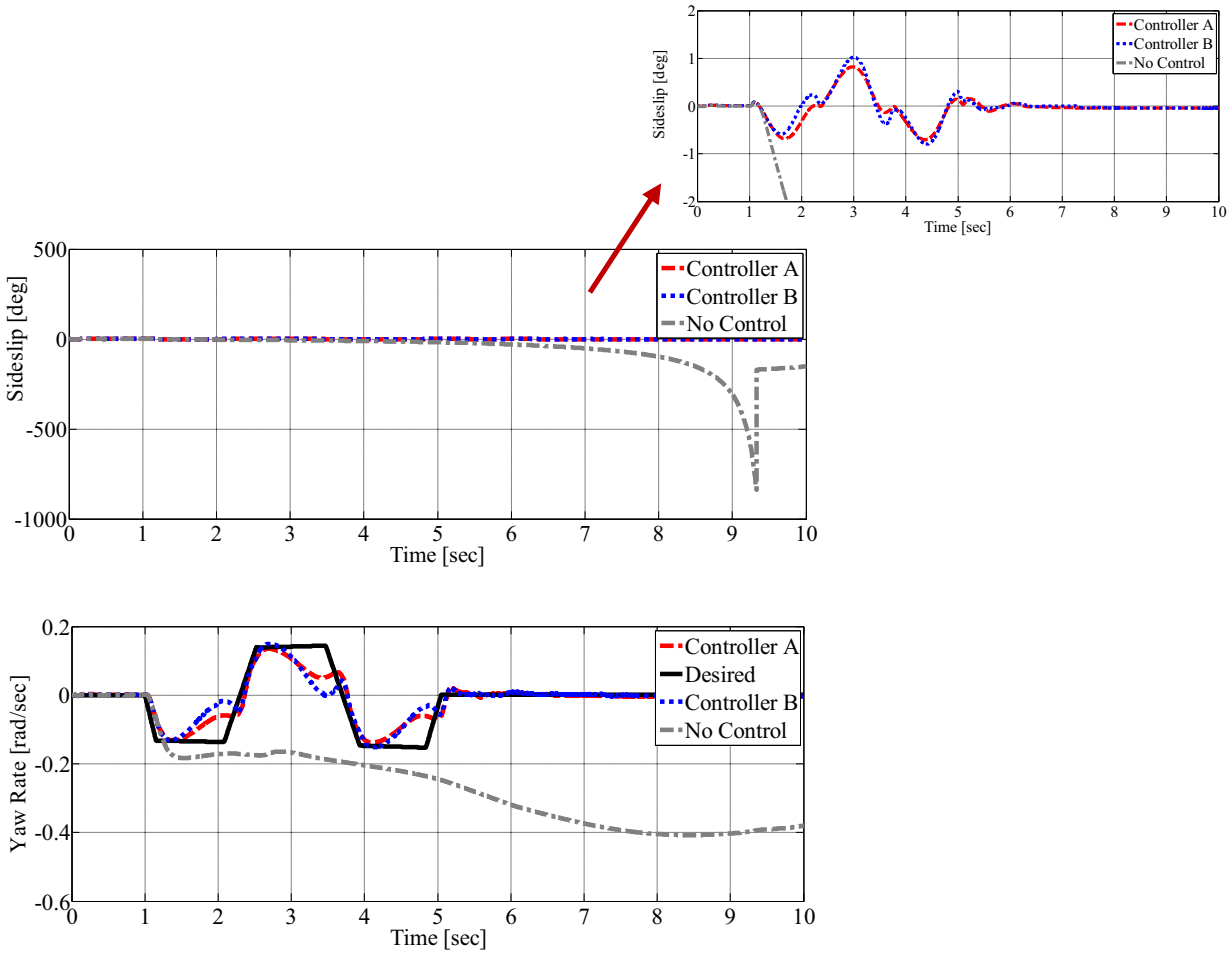

Fig. 7. Comparison of sideslip and yaw rate tracking performance with controllers A and B.

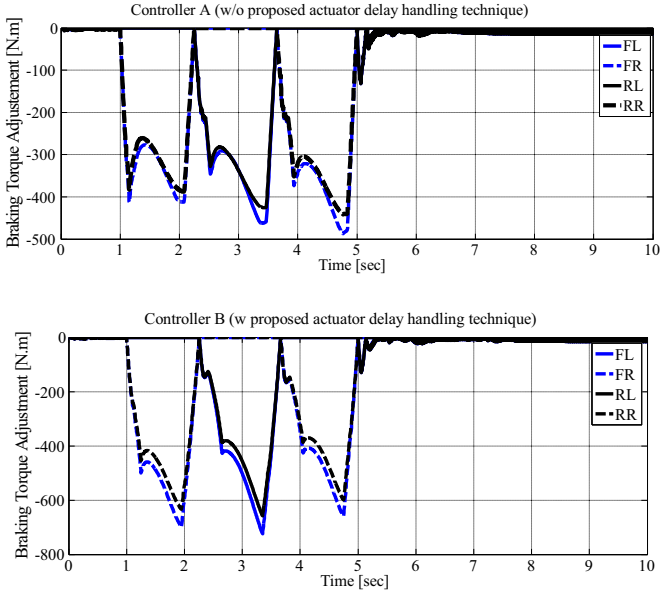

Fig. 8. Comparison of braking torque adjustments of controllers A and B.

$$UB = \begin{bmatrix} 0 & 0 & \cdots & 0 \end{bmatrix}^T \tag{37}$$

where Q_{brake}^{max} is maximum brake torque that can be applied to the wheels. The constraints introduced in Eqs. (36) and (37) are considered in optimization result computation with the quadratic performance index in Eq. (18) with $4 \times N$ and $4 \times M$ sizes for controllers A and B, respectively. This Quadratic Programming (QP) problem can be solved using several existing numerical algorithms and toolboxes. In this paper, QPOASES toolbox [27] is used as a numerical method that involve an iteration procedure. Once the optimal control sequence is obtained, the first set of this sequence is applied to the system and the rest are discarded. The optimization problem is repeated at the next sampling with renewed measurements/estimations.

3. Simulation results

In this section, the performance of proposed controllers on handling actuator delay is studied with the help of simulations in CarSim/MATLAB environment. CarSim simulations were performed with a high-fidelity model of GM Equinox to reduce the number of labor-intensive vehicle tests and is to investigate extreme and dangerous driving conditions. This vehicle is a sport utility vehicle equipped with a hydraulic brake system, and Table 1 illustrates its primary properties.

A brake system is considered in the simulations as available actuation system that enables differential negative torque adjustment individually on wheels. Control loop structure is shown in Fig. 3.

The simulation and experimental tests will evaluate the performance of two similar MPC controllers; controllers A and B. Controller A considers actuator delay in prediction model for delay handling, while controller B supervises delay impacts in distribution algorithm only. The

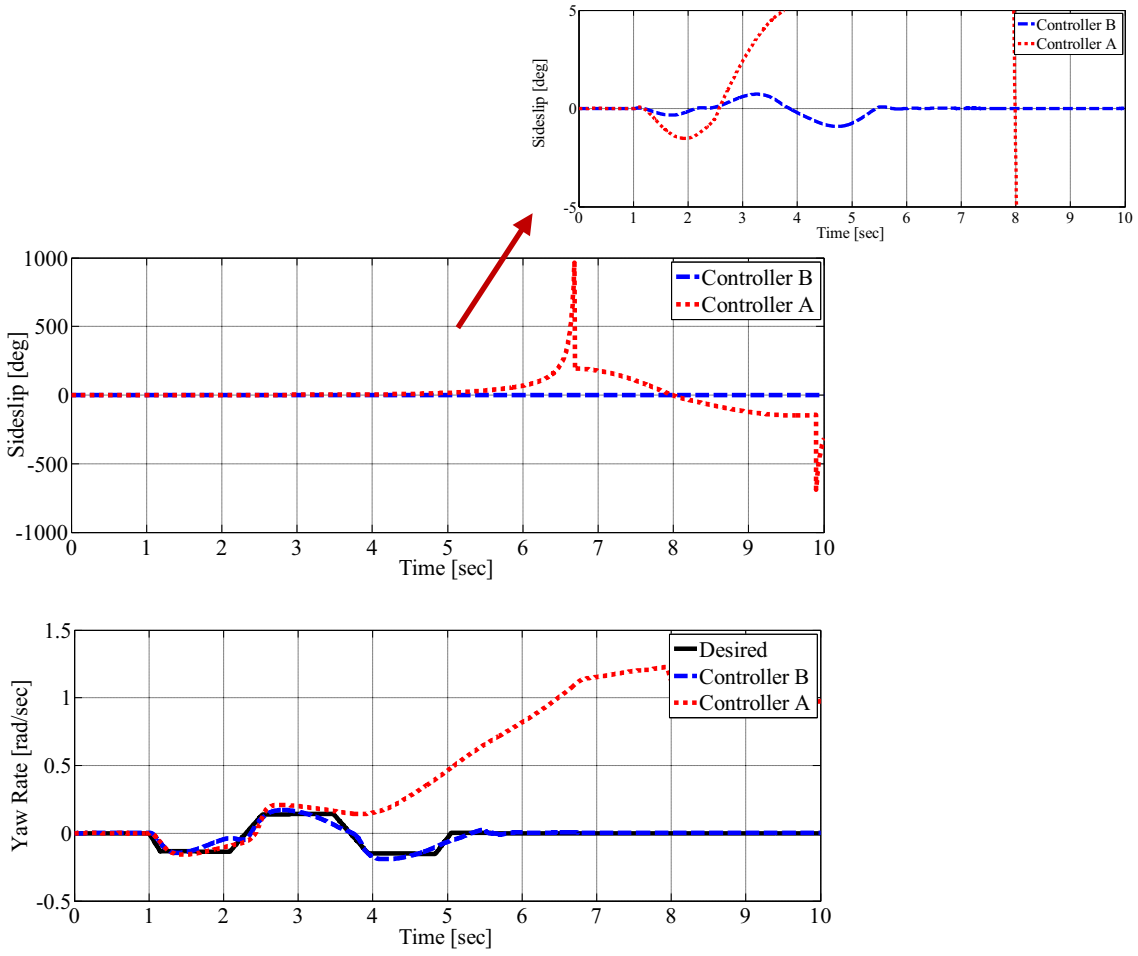

Fig. 9. Comparison of sideslip and yaw rate tracking performance with controllers A and B with a significant actuator delay.

Table 1
Primary vehicle properties.

Symbol	Quantity	Value
m	*Mass*	*2270* kg
L_f	*Distance between CG and front axle*	*1.42033* m
L_r	*Distance between CG and rear axle*	*1.43767* m
R_{eff}	*Tire effective radius*	*0.351* m
I_z	*Moment of inertia about normal axis*	*4600* kg. m^2
ub, lb	*Maximum/minimum braking torque*	*0, −1600* Nm

Table 2
MPC controllers A and B Parameters in simulation.

Symbol	Controller A	Controller B
N	*5*	*5*
M	*N/A*	*10*
T_s	*0.005* s	*0.005* s
Q	$[5 \quad 100 \quad 0 \quad 0 \quad 0 \quad 0] \times I_{6\times6}$	$[5 \quad 100] \times I_{2\times2}$
R	$10^{-6} \times I_{4\times4}$	$10^{-8} \times I_{1\times1}$
S	*N/A*	1
W	*N/A*	$I_{4\times4}$

following flowcharts that describes the real-time control algorithms in controllers A and B, Fig. 4.

The tunings for controllers A and B are listed in Table 2. Capturing the vehicle dynamics with the MPC control modules requires that the prediction horizon *N* be of sufficient length. However, the control horizon is not typically chosen to be large for two major reasons. First, the resultant computational burden and challenges in real time implementation, and second, the non-predictable driver steering command (for non-autonomous driving applications). The simulations and experimental results performed during the tuning phase of the controller indicated that the control horizon and sampling time presented below produce a satisfactory prediction of the vehicle's dynamic response resulting in proper performance of the controllers. A similar methodology is used to tune *M*, however, actuator dynamics determines required preview points in this case, and a larger *M* does not affect the computational complexity remarkably as the MPC prediction model is intact.

A double-lane-change scenario is simulated to compare the performance of controllers A and B. Fig. 5 depicts the driver steering command and lateral acceleration during the scenario. As can be seen, the maximum lateral acceleration achieved on CarSim-generated surface is approximately 0.2 that represents a very slippery road condition. Driving scenario starts with entry speed of 100 km/h without any acceleration. This maneuver is a standard ISO test to evaluate handling performance and is generally exploited as a fundamental part of the vehicle design procedure and assessment [28]. An artificial delay emulating actuator lag is applied to the controller output in simulations. Delay in reaching target brake pressure is considered as a first-order delay shown in Fig. 6.

Fig. 7 illustrates the sideslip angle and yaw rate tracking performance with two controllers A and B, and no control case. Controllers A and B can predict the actuator delay with the proposed control techniques and are prosperous in delay compensation and vehicle stabilization with sideslip angles less than 1° approximately. The yaw tracking performance of controllers are similar and confer a satisfactory transient response with minor tracking errors. The control adjustments of con-

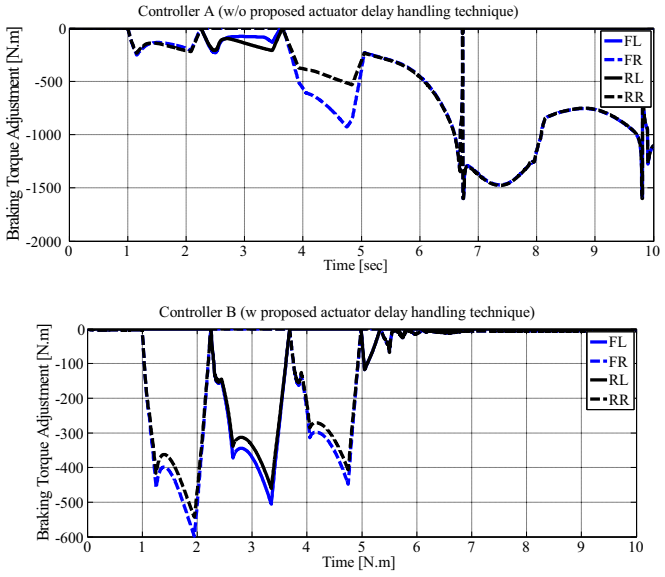

Fig. 10. Comparison of braking torque adjustments of controllers A and B with a significant actuator delay.

trollers A and B are shown in Fig. 8. In case of over-steer or under-steer conditions, required torque correction is generated via brake system on the left or right wheels, respectively to diminish the actual and desired dynamic behaviors discrepancies. In a contrast to controlled event, vehicle was not capable of following desired yaw rate after the driver counter-steering command to the left without controller. As a result, sideslip angles gradually increase in magnitude and exceed over-limit values implying an unstable condition. From the aforementioned simulation results, controllers A and B show a pleasing handling performance in presence of actuator delay in a severe driving scenario, where the passive vehicle cannot be stable.

In order to test the performance capabilities of controllers A and B in actuator delay compensation, a similar maneuver is repeated in simulation with a much lagged actuator. The driver steering command, road condition, and vehicle entry speed are unchanged. For simulation purposes, twice a first-order delay shown in Fig. 6 is considered. Fig. 9 shows vehicle sideslip angle and yaw rate performance with controllers A and B. It can be seen; controller A is not successful in stabilizing the vehicle and it is diverging from the desired yaw rate with increasing amplitude after 3rd second of driving scenario. The reason may be due to unforeseen actuator dynamic behavior using identical prediction window with a faster actuator scenario. A comprehensive transient behavior of the control action with a more sluggish actuator cannot be captured in prediction model of controller A. In this controller, increasing number of prediction horizon may engender a high computational complexity and a non-real time implementable controller. On the other hand, prediction model of controller B excludes actuator delay, and uses proposed delay handling technique in control action distribution. The outcome of such a control technique is adequate sideslip and yaw tracking responses. Torque adjustments by two controllers are shown in Fig. 10. Although controller A requests a large amount of braking torque, it is not successful in maintaining vehicle stability. Whereas, controller B with appropriate actuator dynamics forecast applies sufficient torque adjustment and holds the vehicle within safe bounds.

4. Experimental results

For real-time performance evaluation of controllers A and B, a GM RWD Equinox illustrated in Fig. 11(a) is used. This vehicle is equipped with a hydraulic brake system that allows a negative differential torque adjustment to enhance handling performance and maintain lateral stability. In the experimental setup, RT2500 shown in Fig. 11(b), is uti-

Fig. 11. (a) GM RWD Equinox platform equipped with differential braking system (b) RT system.

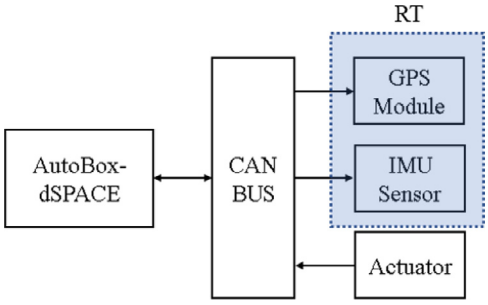

Fig. 12. Experimental setup for controller real-time implementation.

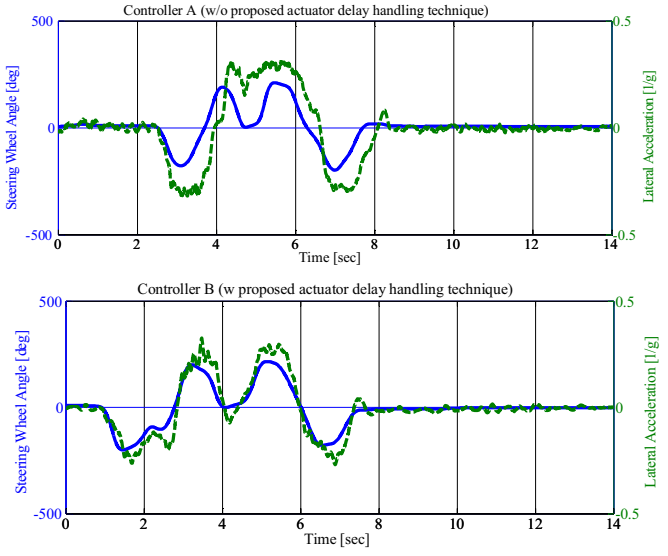

Fig. 13. Driver Steering command and lateral acceleration (experiment).

lized to update the prediction model parameters that combines the high data rate and robustness of inertial navigation systems. Furthermore, a dSPACE AutoBox is employed for proposed controller implementation, as can be seen in Fig. 12. Due to actuation system dynamics, requested and delivered control actions may not be identical. Similar to computer-aided simulations, aforementioned distinction is modeled throughout a first-order delay with time constant of 75 ms in real-time prototyping according to actuator response in experiments. Although a high-fidelity CarSim vehicle model is utilized, the simulated vehicle dynamic response may vary slightly from actual one due to possible simplifications and unmodeled dynamics. Therefore, the tuning matrices Q and R may be different in experimental tests and are shown in Table 3.

The experimental driving scenario involves a double lane change maneuver with entry speed of approximately 50 km/h on slippery road condition. A professional driver performed the experiments without

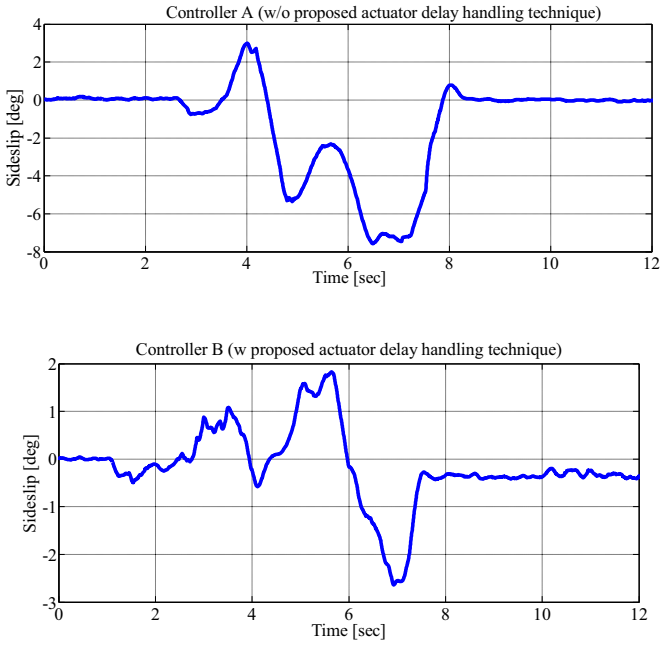

Fig. 14. Comparison of sideslip control performance with controllers A and B (experiment).

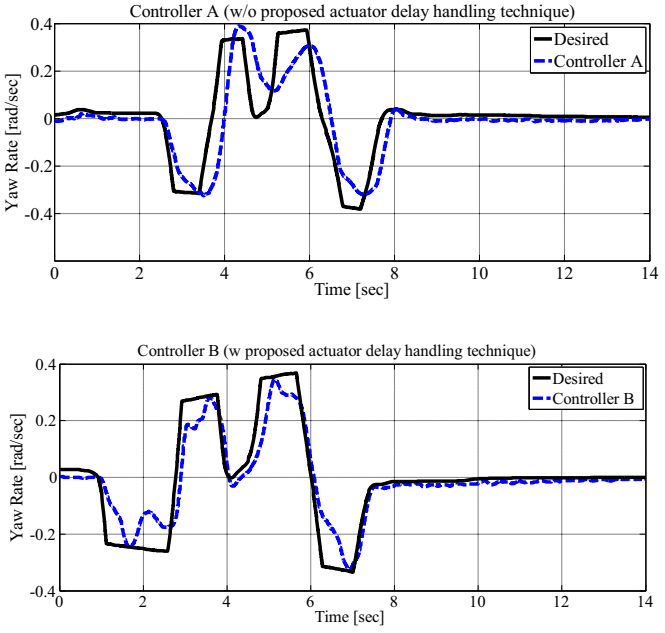

Fig. 15. Comparison of yaw rate tracking performance with controllers A and B (experiment).

Table 3
MPC Controllers A and B Parameters in experiment.

Symbol	Controller A	Controller B
N	*5*	*5*
M	*N/A*	*10*
T_s	*0.005* s	*0.005* s
Q	$[5 \quad 150 \quad 0 \quad 0 \quad 0 \quad 0] \times I_{6\times6}$	$[5 \quad 150] \times I_{2\times2}$
R	$3 \times 10^{-6} \times I_{4\times4}$	$6 \times 10^{-8} \times I_{1\times1}$
S	*N/A*	1
W	*N/A*	$I_{4\times4}$

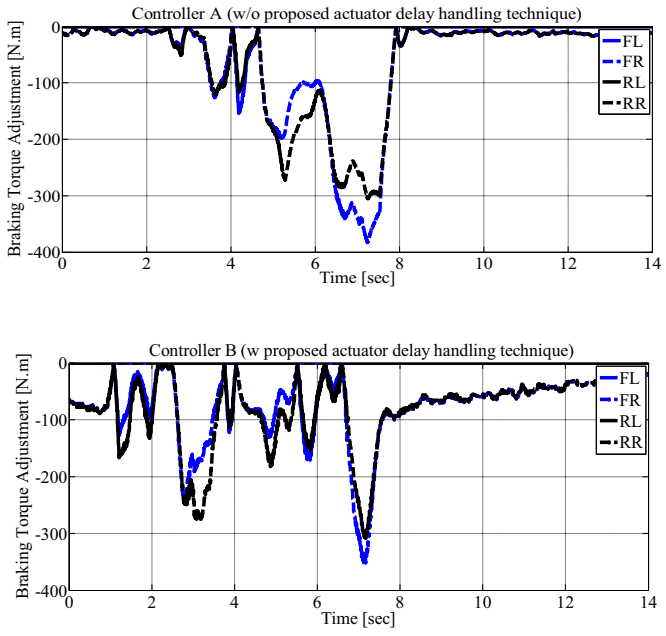

Fig. 16. Comparison of braking torque adjustments of controllers A and B (experiment).

gas/brake pedal engagement. For a legitimate performance comparison of controllers A and B, consistent steering input is crucial. Fig. 13 shows the applied steering angle and resultant lateral acceleration that declares similar test conditions for controllers A and B. The maximum lateral acceleration in both experiments is about 0.3 g ($g = 9.81 m/s^2$) representing a harsh driving situation.

Fig 14 shows the sideslip control performance of controllers A and B. The vehicle reported response after the first lane change entails a particular attention, since vehicle stability may be endangered due to another counter-steer action. It can be observed that with controller A, maximum sideslip angle is about 9°; however, with controller B it is about 3°. The superiority of the proposed actuator delay handling technique is more evident in Fig. 15, where the yaw tracking performances are compared. It can be seen that the vehicle yaw rate response with controller A deviates from the desired signal noticeably around 4–6 s of driving scenario, whereas with controller B, desired signal could be followed without a significant error. Prediction window extension for a better actuator dynamic behavior anticipation is feasible in real-time for controller B with low computational burden. Therefore, controller B can calculate a more precise control action for actuator delay compensation. This can be seen in Fig. 16, where braking torque adjustments are shown for controllers A and B. Although after the first lane change (5 to 8 s), escalation of error between actual and desired vehicle states results in larger torque adjustments with controller A, it could not prevent a delayed intervention. In a similar set of driver inputs, controller B has developed an immediate torque adjustment to counterbalance actuator lag. This indicates that with equal number of predictions in model predictive controllers A and B, controller B can produce a more in phase control adjustment with actuator delay handling technique in distribution, while controller A is belated in generating mandatory control adjustments.

5. Conclusion

In this paper, a predictive technique was proposed to counteract actuator delay in vehicle stability control. The proposed technique is used to design a model predictive control structure that is implantable in real-time with a precise anticipation of actuator dynamics. In this technique, size of the system prediction model is not expanded, and actuator dynamic model is considered as a part of control action distribution method. Thus, online computational load is slightly influenced and a

competent candidate of a low-cost delay handling method is introduced for industrial applications. In addition, the proposed technique is not constrained to neither vehicle stability control nor particular actuator and can be applied to a broad class of model predictive control applications with recognized actuator delays. The performance of the proposed controller is investigated through computer-aided simulations. The controlled vehicle response in a double lane change maneuver performed in MATLAB/CarSim environment demonstrated that the proposed delay handling technique can enhance the stability control proficiency in case of considerable actuator delay. Furthermore, experimental evaluations have been accomplished on a SUV that shows effectiveness of the proposed development in control action allocation and confirmed the computer simulation inquires.

Acknowledgment

Authors would like to show their gratitude to General Motors, Automotive Partnership Canada (APC), and Ontario Research Fund (ORF) for all financial and technical supports during this research.

References

[1] Jalali Kiumars, et al. Development of an advanced torque vectoring control system for an electric vehicle with in-wheel motors using soft computing techniques. SAE Int J Altern Powertrains 2013;2(2):261–78.
[2] Lyckegaard A, Hels T, Bernhoft IM. Effectiveness of electronic stability control on single-vehicle accidents. Traffic Inj Prev 2015;16(4):380–6.
[3] Høye A. The effects of Electronic Stability Control (ESC) on crashes—an update. Accid Anal Prev 2011;43(3):1148–59.
[4] Canale M, Fagiano L, Signorile MC. A model predictive control approach to vehicle yaw control using identified models. Proc Inst Mech Eng Part D J Automob Eng 2012;226(5):577–90.
[5] Liu P, Ozguner U. "Distributed model predictive control of spatially decoupled systems using switched cost functions," arXiv Prepr. arXiv1606.02224, 2016.
[6] Bemporad A, Morari M. Robust model predictive control: a survey. In: Robustness in identification and control. Springer; 1999. p. 207–26.
[7] Falcone P, Borrelli F, Tseng HE, Asgari J, Hrovat D. Linear time-varying model predictive control and its application to active steering systems: stability analysis and experimental validation. Int J Robust Nonlinear Control 2008;18(8):862–75.
[8] Singh L, Fuller J. Trajectory generation for a UAV in urban terrain, using nonlinear MPC. In: American Control Conference, 2001. Proceedings of the 2001, 3; 2001. p. 2301–8.
[9] Falcone P, Borrelli F, Asgari J, Tseng HE, Hrovat D. Predictive active steering control for autonomous vehicle systems. IEEE Trans Control Syst Technol 2007;15(3):566–80.
[10] Borrelli F, Falcone P, Keviczky T, Asgari J, Hrovat D. MPC-based approach to active steering for autonomous vehicle systems. Int J Veh Auton Syst 2005;3(2–4):265–91.
[11] Asgari J, Hrovat D. Potential benefits of Interactive Vehicle Control Systems. Intern Rep 2002.
[12] Bemporad A, Rocchi C. Decentralized linear time-varying model predictive control of a formation of unmanned aerial vehicles. In: Decision and control and European control conference (CDC-ECC), 2011 50th IEEE Conference on; 2011. p. 7488–93.
[13] Falcone P, Tufo M, Borrelli F, Asgari J, Tseng HE. A linear time varying model predictive control approach to the integrated vehicle dynamics control problem in autonomous systems. In: Decision and control, 2007 46th IEEE conference on; 2007. p. 2980–5.
[14] Barbarisi O, Palmieri G, Scala S, Glielmo L. LTV-MPC for yaw rate control and side slip control with dynamically constrained differential braking. Eur J Control 2009;15(3–4):468–79.
[15] Cortes P, Rodriguez J, Silva C, Flores A. Delay compensation in model predictive current control of a three-phase inverter. IEEE Trans Ind Electron 2012;59(2):1323–5.
[16] Su Y, Tan KK, Lee TH. Computation delay compensation for real time implementation of robust model predictive control. J Process Control 2013;23(9):1342–9.
[17] Liu J, Jayakumar P, Stein JL, Ersal T. A multi-stage optimization formulation for MPC-based obstacle avoidance in autonomous vehicles using a LIDAR sensor. Ann Arbor 2014;1001:48109.
[18] Rajamani R. Vehicle dynamics and control. Springer Science & Business Media; 2011.
[19] Rezaeian A, et al. Novel tire force estimation strategy for real-time implementation on vehicle applications. IEEE Trans Veh Technol 2015;64(6):2231–41.
[20] Bingulac S, Vanlandingham HF. Discretization and continualization of mimo systems. Yugosl J Oper Res 1994;4(7):27–34.
[21] Venkatasubramanian V, Rengaswamy R, Yin K, Kavuri SN. A review of process fault detection and diagnosis: Part I: quantitative model-based methods. Comput Chem Eng 2003;27(3):293–311.
[22] Borrelli F, Bemporad A, Morari M. Predictive control for linear and hybrid systems. Cambridge University Press; 2017.
[23] Hashemi E, et al. Integrated estimation structure for the tire friction forces in ground vehicles. In: Advanced Intelligent Mechatronics (AIM), 2016 IEEE international conference on; 2016. p. 1657–62.
[24] Chen S-K, Ghoneim Y, Moshchuk N, Litkouhi B, Pylypchuk V. Tire-force based holistic corner control. In: ASME 2012 International mechanical engineering congress and exposition; 2012. p. 133–40.
[25] Pylypchuk V, Chen S-K, Moshchuk N, Litkouhi B. Slip-based holistic corner control. In: ASME 2011 international mechanical engineering congress and exposition; 2011. p. 337–42.
[26] Kasinathan D, Khajepour A, Chen S-K, Litkouhi B. "Constrained holistic

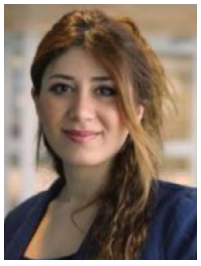

Asal Nahidi received her Ph.D. degree in Mechanical and Mechatronics Engineering at University of Waterloo, Waterloo, ON, Canada. She followed her interests in Vehicle Dynamics and Controls as a postdoctoral fellow in Mechatronic Vehicle Systems Lab and then joined General Motors Canada as a Vehicle Dynamics Specialist. She has more than 5 patents in the filed of Vehicle Dynamics and Chassis Controls. Her research interests also include Robust Control, Fault Tolerant Control, Optimization, Modelling, Vibration, and Acoustics.

Amir Khajepour is currently a Professor of Mechanical and Mechatronics Engineering with the University of Waterloo, Waterloo, ON, Canada, and the Canada Research Chair in Mechatronic Vehicle Systems. He has developed an extensive research program that applies his expertise in several key multidisciplinary areas. His research interests include System Modeling and Control of Dynamic Systems. His research has resulted in several patents and technology transfers. He is the author of more than 250 journal and conference publications and four books. Prof. Khajepour is a Fellow of the American Society of Mechanical Engineers and the Canadian Society of Mechanical Engineering. He has received three Best Paper Awards.

Alireza Kasaeizadeh is working with General Motors research and development at Warren Technical Center, (Warren, MI, USA) as a Senior Researcher in the field of Automated Driving and Vehicle Control. He is also Adjunct Professor at University of Waterloo, Waterloo, ON, Canada where he got his Ph.D. in Mechanical Engineering followed by two years postdoctoral fellowship and one year of serving as Research Assistant Professor. He holds BSc. and MSc. degrees from Sharif University of Technology, Tehran, Iran. He has more than 25 journal and conference papers in addition to 5 patents. He also has more than 15 years of industrial experiences in automotive industry and in particular, Active Safety System, Chassis Control System Design and Field-Testing. His major field of interest is Automated Driving, Vehicle Dynamics, Control and Optimization.

Shih-Ken Chen received the B.S. degree from National Taiwan University, Taipei, Taiwan, in 1985 and the M.S. degree from the University of Wisconsin, Madison, in 1990 and the Ph.D. degree from Massachusetts Institute of Technology, Cambridge, in 1996, both in Mechanical engineering. He then joined the Research and Development Center of General Motors (GM) Corporation. He is currently a Staff Researcher with the Global R&D Center, GM, Warren, MI. His previous research interests include Collision Avoidance Systems, Electronic Stability Control, Active All-wheel-steer Control, and Rollover Avoidance. His current research interests include integrated Chassis and Vehicle Control for both conventional and electric drivelines, driver-in-the-loop vehicle control, and vehicle active safety systems.

Bakhtiar Litkouhi received the B.Sc. degree in Mechanical Engineering, the M.Sc. degree in applied mathematics, and the Ph.D. degree in systems science, specializing in controls. He was an Assistant Professor with Oakland University, Rochester, MI. He was the Acting Director with the Electrical and Controls Integration Laboratory, Global Research and Development Center, General Motors Company, Warren, MI. He was a Program Manager for several large-scale projects on intelligent vehicle systems, human–machine faces, systems engineering, and integrated vehicle control, where he has made many contributions through numerous patents, publications, and presentations. He is currently the Manager of perception and vehicle control systems with the Global Research and Development Center. He is also a Program Manager with the General Motors–Carnegie Mellon University Autonomous Driving Collaborative Research Laboratory and a member of the Board of Directors with the Waterloo Center for Automotive Research. Dr. Litkouhi is a board member of the Intelligent Transportation Society of Michigan.